International Journal of Pharmaceutics 393 (2010) 88–95

Contents lists available at ScienceDirect

International Journal of Pharmaceutics

journal homepage: www.elsevier.com/locate/ijpharm

A centrifuge method to measure particle cohesion forces to substrate surfaces: The use of a force distribution concept for data interpretation

Thanh T. Nguyen[a,*], Clinton Rambanapasi[a], Anne H. de Boer[a], Henderik W. Frijlink[a], Peter M.v.D. Ven[b], Joop de Vries[c], Henk J. Busscher[c], Kees v.D. Voort Maarschalk[a,d]

[a] Department of Pharmaceutical Technology and Biopharmacy, University of Groningen, Groningen, The Netherlands
[b] TNO Quality of Life, Zeist, The Netherlands
[c] Department of Biomedical Engineering, University Medical Centre Groningen, Groningen, The Netherlands
[d] Oral and Polymeric Products Development Department, Schering-Plough, Oss, The Netherlands

ARTICLE INFO

Article history:
Received 6 October 2009
Received in revised form 9 April 2010
Accepted 12 April 2010
Available online 20 April 2010

Keywords:
Cohesion force
Adhesion force
Dry powder mixtures
Centrifuge method
Force distribution concept
Atomic force microscope

ABSTRACT

Adhesion, agglomeration and de-agglomeration of micronized particles and larger carrier particles are of special importance during manufacturing of pharmaceutical products when the inherent cohesion property of fine particles challenges the content uniformity of dry mixtures. To characterize particle–particle adhesion, measurements with atomic force microscopy (AFM) and a centrifuge method were performed using microcrystalline cellulose as model material. The variations in AFM measurements were too large to draw a conclusion. A force distribution concept (FDC) was used in the interpretation of the results from the centrifuge method. This solved the problem of variation caused by the polydispersity of the sample and enabled quantitative characterization of the particle adhesion. An experimental design was used to investigate the effect of the 'press-on force', 'press-on time' and surface roughness. All these factors were shown to have an effect although the effect of press-on force and press-on time was merely distinguishable as a quadratic effect.

1. Introduction

Oral solid dosage forms are by far the most popular dosage forms in today's pharmaceutical industry. The hydrophobic nature of many active pharmaceutical ingredients (APIs) requires their formulation as microsized or even nanosized particles. However, the fine particle size causes serious challenges for manufacturers related to poor powder flow, product dispersion and end product homogeneity (Saunders, 1991). Fine APIs are highly susceptible to agglomeration due to the important increase in the balance of API cohesion relative to the API's gravity. In this paper, the term cohesion is used to denote the adhesion between particles of the same material, the term adhesion is used more generally to denote interaction between particles of either the same material or different materials. In practice, agglomerates of fine particles are often found on the top of the powder beds after blending, leading to a non-uniform blend which causes high variation in drug concentration after granulation or a non-uniform API distribution after unit dose production. A pragmatic solution to the problem is the application of shear-intensifying equipment such as choppers during blending. However, the fine components in a formulation have an inherent propensity to form agglomerates, so shear intensification alone is not enough to prevent the re-formation of agglomerates after blending. The concept of ordered mixing (Hersey, 1975) and cohesive–adhesive balance introduced recently in the field of dry powder inhaler formulation (Begat et al., 2004) are of special interest in fine particles blending. Only a fundamental understanding of adhesion properties of agglomerated particles enables the design and development of an adequate formulation and choice of appropriate process condition.

A number of theories have been developed to describe and to estimate the adhesion forces between particles, both qualitatively and quantitatively (Hamaker, 1937; Dzyaloshinskii et al., 1961; Derjaguin et al., 1975; Johnson et al., 1971). However, these theories fail to explain or predict the behavior of real powders because of inappropriate assumptions regarding for example, the particle shape in calculating the area of contact between interacting bodies. These contact areas are the areas where the materials of the interacting bodies are close to each other, usually in the Ångstrom range (10^{-10} m). An error in contact area estimation may lead to significant error in the adhesion force calculated. A spherical particle is usually taken to estimate the contact area. However, APIs exist in various shapes which makes it difficult to calculate the contact area and hence, the force of adhesion. Additionally, sur-

* Corresponding author. Tel.: +31 50 363 3282; fax: +31 50 363 2500.
E-mail address: t.t.nguyen@rug.nl (T.T. Nguyen).

0378-5173/$ – see front matter © 2010 Elsevier B.V. All rights reserved.
doi:10.1016/j.ijpharm.2010.04.016

faces of API particles are normally not smooth; the asperities on the surfaces may become even more important than the particles in adhesion interaction (Rumpf, 1990). Especially when 'load' or 'press-on' conditions exist, the pressure concentrated on tiny surface area of asperities may influence significantly the adhesion force between two bodies. The natural variation in particle's surface roughness makes the theoretical prediction of adhesion force practically impossible. Furthermore, existing theories deal only with mono disperse particles; the whole particle size distribution is never taken into account which is not appropriate concerning real powders.

Beside theoretical calculations, experimental methods have been developed to measure adhesion interaction between particles (Zimon, 1982b). The introduction of the atomic force microscope (AFM) has made it possible to measure adhesion forces as small as 10^{-18} N from a distance as close as 1 Å (Binnig et al., 1986). By using a colloidal probe mounted on an AFM cantilever, adhesion interaction between two particles or a particle and a surface can be directly measured without any assumption concerning particle size, shape and surface roughness. However, it is only possible to perform AFM measurements with one single particle at a time and considerable efforts are needed to characterize a polydisperse powder with a certain size and surface variation within the sample.

Among other methods, the centrifuge method has been introduced in the 1960s (Krupp, 1967) and has been extensively used by researchers for measurement of adhesion strengths between particles and surfaces (Salazar-Banda et al., 2007, Lam and Newton, 1991, Podczeck and Newton, 1995). The advantage of the centrifuge method is the possibility to measure the interaction of a relatively large number of particles with a surface in a single experiment, and hence may yield a statistically more representative value for the entire powder under consideration.

In principle, the method uses a centrifugal force to separate adhering particles from a substrate surface. The centrifugal force is oriented perpendicularly to the contact surface of two interacting bodies, in opposite direction of the adhesion force between particle and surface. The particles are detached from the surface when the magnitude of centrifugal force exceeds the magnitude of adhesion force. The centrifugal force applied to a particle during centrifugation is proportional to the first power of particle mass (m) and centrifugal radius (R_C) and to the second power of angular velocity (ω) as shown in Eq. (1)

$$F_C = m.\omega^2.R_C \quad (1)$$

The adhesion force can be calculated based on the retention curve which plots the percentage of particles left on the surface as function of the centrifugal force. The force necessary to detach 50% of particles from the substrate surface is often used to represent the adhesion force of the particles to the surface (Lam and Newton, 1991, Podczeck and Newton, 1995). With a polydisperse sample, the use of centrifuge method to study a large number of particles includes a challenge with regard to data interpretation. Since the particles studied have different sizes, the use of only one representative particle size (usually median particle size) to calculate the centrifugal force is not rational. For a particle with known shape, the volume and mass of the particle are proportional to the third power of the characteristic size of the particle such as particle diameter (d_v: diameter of a sphere having the same volume) and the first power of particle's true density (ρ) as shown in Eq. (2)

$$m = \rho.\frac{\pi.d_v^3}{6} \quad (2)$$

As a result, the centrifugal force is proportional to the third power of the particle size and is sensitive to alterations in particle size. While studying particle adhesion using the centrifuge method, a small variation in particle size will lead to high variations in the calculated centrifugal force, and consequently also in the adhesion force derived thereof.

A force distribution concept (FDC) had been introduced by De Boer et al. (2003) to characterize the performance of dry powder inhalation formulations with air classifier technology. In this paper, the force distribution concept is applied in the interpretation of cohesion interaction of fine particles which are susceptible to agglomerate formation during dry blending. Microcrystalline cellulose (MCC) was used as a model material to study the cohesion of MCC particle and MCC surface.

2. Materials and methods

2.1. Preparation and characterization of particle size fraction

Microcrystalline cellulose (Avicel® PH-101 and Avicel® PH-105) was kindly supplied by FMC Biopolymer (Wallingstown, Ireland).

A particle fraction with a size range from 38 to 53 μm was prepared by double sieving Avicel® PH-101 (sample size 100 g) using subsequently a vibratory sieve (Retsch AS200, Retsch, Haan, Germany) and an air jet sieve (Alpine Augsburg, Germany). Particles of this size fraction were used as adhering particles in the centrifuge method.

A particle fraction with a size range from 100 to 160 μm was prepared from Avicel® PH-105 in a similar way. This size fraction was used to make tablets with 'rough' surfaces.

The size fraction less than 38 μm from Avicel® PH-101 was used to make tablets with 'smooth' surfaces.

The particle size distribution of 38–53 μm fraction was characterized by laser diffraction using a HELOS MODEL KA (Sympatec GmbH, Clausthal-Zellerfeld, Germany). A RODOS dry powder dispenser (Sympatec) was used to disperse the powder into primary particles at 4 bar air pressure.

The number distribution of volume equivalent diameter was calculated based on the laser diffraction results. The first 0.65% of the distribution (0.9–9 μm) in the laser diffraction result was omitted from the number distribution calculations because it is of a size that cannot be observed visually using optical microscopy. The particle size distribution in volume and in number is shown in Fig. 1.

2.2. Preparation and characterization of substrate surface

Substrate surfaces of different surface porosities were prepared by compacting particles of different size fractions under the same compaction pressure. The size fraction from 100 to 160 μm was used to compress tablets with 'rough' surfaces and the size fraction less than 38 μm was used to compress tablets with 'smooth' surfaces. A quantity of 300 mg of powder was filled into a 15 mm non-lubricated die and compressed into round, flat tablets using a

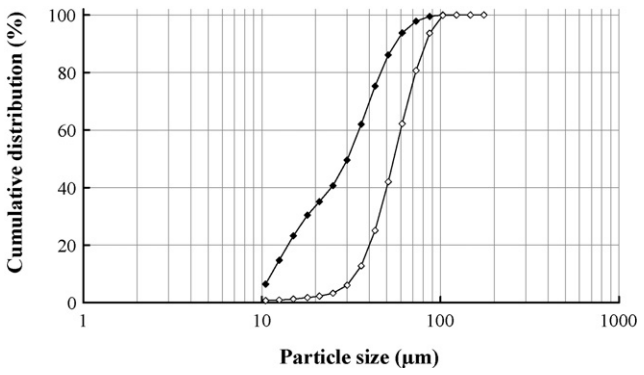

Fig. 1. Particle size distribution of the 38-53 μm fraction. Open symbol: volume distribution. Solid symbol: number distribution.

ESH hydraulic press (Hydro Mooi, Appingedam, The Netherlands). The maximum compaction pressure of 170 MPa was reached in 6 s.

The substrate with deposited particles on the surface was observed visually with an optical microscope ELV: 78952 (ELV, Leer, Germany) and scanning electron microscope (SEM) (JEOL JSM-6301F microscope, Jeol, Japan). Surfaces without deposited particles were also scanned to analyze for surface area of troughs found on that substrate surface. Image analysis was done using ImageJ software (http://rsbweb.nih.gov/ij/). A Gaussian filter (sigma = 2 pixels) was applied before making the image binary. 8 bit SEM images were made binary using Isodata threshold algorithm (Young et al., 1995). The 'surface porosity' (i.e. the relative area of troughs) was then calculated as the percentage of surface area of troughs in the total scanned area as shown in Eq. (3)

$$\text{surface porosity} = \frac{\text{total surface area of troughs}}{\text{total scanned area}} \times 100\% \quad (3)$$

2.3. Cohesion force measurement by atomic force microscope (AFM)

Cohesion forces between MCC particles (38–53 μm) and MCC surfaces were measured using a Nanoscope V AFM (Veeco Instrument, Santa Barbara, CA) operating in "Contact" mode. The colloidal probes were prepared by gluing MCC particles on tipless AFM cantilevers according to the procedure described by (Busscher et al., 2008). Briefly, the MCC particles of 38–53 μm size fraction were deposited on a glass slice, a tipless AFM cantilever (μmasch CSC12, MikroMasch, Estonia) which was brought in contact with a freshly prepared two components epoxy resin (Kombi Turbo, Bison International, Goes, The Netherlands) was gently introduced to the glass slice with help of a micromanipulator (Narishige, Narishige International USA, Inc., East Meadow, NY) to pick up one particle. The colloidal probe was kept overnight allowing the glue mixture to solidify. Before mounting the particles, the spring constant of tipless cantilevers was determined using the thermal method described (Hutter and Bechhoefer, 1993). Two colloidal probes were prepared, the cohesive interaction forces were measured between two MCC particles and two tablets of 'rough' surface, two tablets of 'smooth' surface. For each particle–surface interaction, measurements were done at five different positions and repeated ten times at each point.

2.4. Cohesion force measurement by the centrifuge method

Modified centrifuge tubes were designed and constructed at the University of Groningen. This tube has three parts as illustrated in Fig. 2. A holding tube (Fig. 2A), the substrate holding plate (Fig. 2B), and a recipient chamber to collect the detached particles (Fig. 2C). These tubes were designed to be used in a Hettich Rotanta D-7200 centrifuge (Hettich AG, Switzerland) with adjustable centrifugal speed up to 4000 rotations per minute (rpm). With this design, it is possible to turn the substrate holding plate in two opposite directions, placing the particle on the substrate surface under two different centrifugal forces of opposite directions. When facing the particles inward the centrifugal axis, the centrifugal force is applied in the same direction with adhesion force which presses the particles on the surface, strengthening the interaction. In this direction, the centrifugal force is called the 'press-on' force. When facing the particles outward the centrifugal axis, the centrifugal force is applied in the opposite direction of adhesion force. The adhering particles detach when the centrifugal force exceeds the adhesion force in magnitude. This force is called the 'spin-off' force.

As the centrifugal force is calculated based on the particle size and particle's true density, deposition of primary particles onto the substrate surface is critical. A small amount of microcrystalline cellulose (hundreds of particles) 38–53 μm in size, was deposited onto the substrate surface by gently sprinkling from a spatula over the MCC compacted surface.

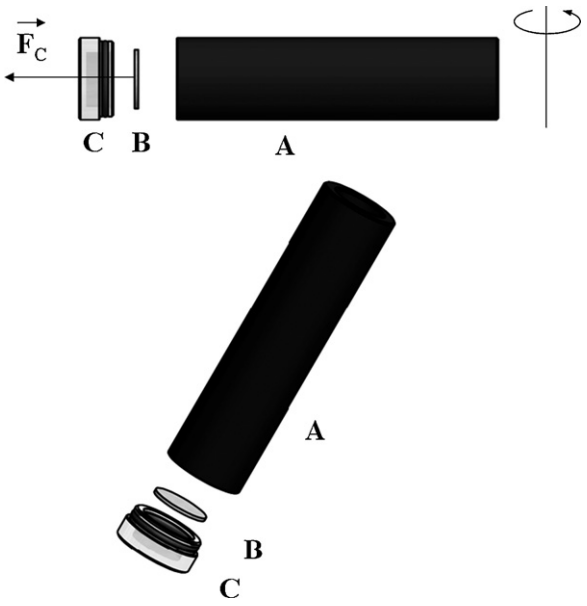

Fig. 2. Modified centrifuge tube used in this study. (A) Holding tube. (B) Substrate holding plate. (C) Recipient chamber to collect the detached particles.

Before deposition, the powders and tablets were kept in closed glass vials at laboratory condition. During the experiments, the temperature was stable at 20 ± 1 °C, the relative humidity varied between 35% and 45%.

After deposition, the particles were subjected to different press-on forces to the surface. The effect of press-on force and press-on time was investigated at three different levels: 1000, 2000 and 3000 rpm of press-on speed and 5, 10 and 15 min of press-on duration.

To eliminate the possible effect of electrostatic forces, the MCC particles deposited on the substrate surface were kept overnight in a humidity controlled chamber of about 30% RH at 20 °C (saturated solution of calcium chloride).

Detachment of particles from the substrate surface was studied by turning the substrate outward the centrifugal axis and centrifuge at five incremental speeds: 1000, 1500, 2000, 3000 and 4000 rpm during 15 min. After each rotation experiment, the substrates with adhering particles were investigated under an optical microscope. Because of the limited contrast between particles and the substrate surface of the same material, a light source was placed parallel to the substrate surface. In this way, adhering particles on the substrate surface became visible under the microscope. Pictures of particles left on the surface were taken after each test. These pictures were used to count the number of particles left on the substrate surface using BacterialCounting software developed by the Groningen University Hospital. In each experiment, the percentage of particles left on the surface was determined at five different 'spin-off' speeds.

2.5. Experimental design and statistics

Twelve experiments were designed to evaluate factors that influence the number of particles left on the surface, which are press-on force (rpm), press-on time, the substrate surface roughness and the interaction between these factors. Details of experimental design and conditions are shown in Table 1. The 12 experiments were run in randomized order and each experiment was carried out with four samples under the same conditions.

Table 1
Experimental design used in the cohesion experiments.

Experiment number	Surface roughness	Press-on force (speed in rpm)	Press-on-time (min)
1	Rough	1000	5
2	Rough	1000	15
3	Rough	3000	5
4	Rough	3000	15
5	Rough	2000	10
6	Rough	2000	10
7	Smooth	1000	5
8	Smooth	1000	15
9	Smooth	3000	5
10	Smooth	3000	15
11	Smooth	2000	10
12	Smooth	2000	10

The detachment data were analyzed by fitting separate regression model for each of the spin-off speed to evaluate the impact of each variable on particle–surface adhesion. Before fitting the models, the surface roughness was coded −1 for the smooth surface and 1 for the rough surface. The lower, intermediate and highest values of press-on force and press-on time were recoded −1, 0 and 1, respectively. In this way, the regression parameters that correspond to the main effects and two-factor interactions can be estimated independently.

The *t*-test for regression coefficients was used to evaluate the main effects and interactions in the regression model.

3. Results and discussion

3.1. Cohesion force measurement by atomic force microscope

Of the two MCC particles used to prepare AFM colloidal probe, there is one particle (called particle 1) smaller than the other (called particle 2). The average cohesive interaction forces (mean ± standard deviation) of particle 1, particle 2 with the rough surfaces are 41.4 ± 18.4 and 81.8 ± 41.7 nN, respectively. The interaction forces of particle 1, particle 2 with the smooth surfaces are 38.3 ± 23.2 and 90.1 ± 40.7 nN, respectively.

The interaction forces range from 11 (minimum) to 147 nN (maximum) with the rough surfaces and from 8 to 168 nN with the smooth surfaces. The difference between rough and smooth surface is not statistically significant ($z = -0.16$, $p = 0.87$, Mann-Whitney U test). Within one position on the substrate surface the force measurement is reproducible: the relative standard variation (RSD) of 10 repeated measurements is less than 5%. However the variation between different measurement positions on the same surface is much higher, RSD ranges from 44% (particle 1 with rough surface) to 60% (particle 1 with smooth surface). This high between-point measurement variation is understandable considering the fact that the surfaces are far from uniform. While moving the MCC probe over a substrate's surface to random positions for adhesion force measurement, there are various possibilities for a particle to come into contact with the surface which is formed by different contact points of different contact areas, leading to large variations in the adhesion force measured. The variations also reflect the natural properties of most of pharmaceutical materials, especially those materials that undergo mechanical size reduction. For this reason, the use of AFM to characterize adhesion properties of a powder sample is fundamentally difficult concerning the large number of particles needed to statistically represent the sample and the delicate manipulation with the micromanipulator to mount particles on AFM cantilevers.

3.2. Cohesion force measurement by the centrifuge method

The detachment results of MCC particles from MCC surfaces are summarized in Table 2, showing the retention (percentage of particles left on the entire surface) after each centrifugal detachment speed. The data represent the average values and standard deviations (SD) of four independent tests carried out at the same conditions.

The cohesion of MCC particles to MCC surfaces depends on several factors (Lam and Newton, 1993; Zimon, 1982a; Lam and Newton, 1991), in this study three frequently documented factors were taken into account in the experimental design: press-on force, press-on time and surface roughness. To identify factors which have a significant effect, a statistical analysis was performed by fitting multivariable linear regression models for each centrifugal detachment speed. The parameters that estimate for the regression model are shown in Table 3. The adjusted R^2 in Table 3 measures how well the model explains the data. R^2 takes the value from 0 to 1, with 1 corresponding to a perfect fit. The R^2 values in Table 3 are low, indicating that the models do not fit the data very well. Therefore, it is important to note that these models should not be used for interpolation. However, the significance of each parameter in the models does explain to which extend the variation of each factor influences the cohesion between particle and surface. It is found that the substrate's surface roughness has significant effect on the percentage of particles left on the surfaces, with a rough surface leading to higher retention at all detachment speeds. The press-on force shows a relatively weak but generally statistically significant effect. The effect of press-on time is only significant at 1000 rpm spin-off speed. According to Zimon (1982a), the distance between asperities of a rough surface affects the particle detachment from the surface. Particles that lay between the asperities, or in troughs, are more difficult to detach than particles lying on top of the asperities.

Table 2
Centrifuge detachment of MCC particles from MCC surfaces.

Experiment number	Percentage of particles left on the surface after centrifugation (%)				
	1000 rpm	1500 rpm	2000 rpm	3000 rpm	4000 rpm
1 (R/1000/5)	82.2 ± 6	67.2 ± 6	53.2 ± 3.6	25.5 ± 4.7	10 ± 2.9
2 (R/1000/15)	74.4 ± 1.9	57.7 ± 4.6	44.3 ± 2	28.4 ± 5.9	9.9 ± 3.2
3 (R/3000/5)	79.7 ± 3.9	63.6 ± 0.7	52 ± 2.1	38.7 ± 6.3	20.1 ± 5.4
4 (R/3000/15)	81 ± 6.4	68.7 ± 9.1	52.5 ± 6.2	39 ± 4.9	19.4 ± 4.4
5 (R/2000/10)	82.3 ± 4.9	65.2 ± 6.5	45 ± 5.9	22.2 ± 8.2	7.9 ± 4.9
6 (R/2000/10)	94.7 ± 0.6	80.5 ± 2.9	67 ± 3.4	27.5 ± 2.9	6 ± 1.3
7 (S/1000/5)	88.8 ± 1.9	59.2 ± 9.4	41.4 ± 4.2	22.7 ± 3.2	10.2 ± 1
8 (S/1000/15)	75.5 ± 5.8	59.4 ± 12.4	49.1 ± 13.2	26.9 ± 5.4	9.3 ± 4.4
9 (S/3000/5)	71.4 ± 6.1	49.8 ± 6	40.2 ± 6.4	19.7 ± 2.9	9.8 ± 2.6
10 (S/3000/15)	67.8 ± 11.7	51.9 ± 11.3	37.9 ± 19.4	22.2 ± 9.5	6 ± 2
11 (S/2000/10)	88.8 ± 2	76.3 ± 3.6	61.9 ± 5.2	32.9 ± 5.1	7.1 ± 2.6
12 (S/2000/10)	75.8 ± 5.2	53.2 ± 11.5	38.8 ± 8.7	20.1 ± 9.6	9.9 ± 5.5

S: smooth surface, R: rough surface/1000, 2000, 3000 rpm/5, 10, 15 min.

Table 3
Parameters estimate for regression models.

Speed (rpm)	1000	1500	2000	3000	4000
Intercept	85.41***	68.81***	53.18***	24.37	7.72***
Surface roughness	2.18*	5.34**	4.53*	3.91***	1.77**
Press-on force	−2.63*	0.18	0.51	2.66*	1.98**
Press-on time	−2.92*	−1.64	−1.51	0.59	−0.67
Surface roughness × press-on time	1.30	0.57	−0.60	0.21	0.50
Surface roughness × press-on force	3.64**	1.65	1.21	3.30*	2.90***
Press-on-time × press-on force	2.35	3.44	1.06	0.92	-0.43
Quadratic effect of press-on time and press-on force (indistinguishable)	−7.82***	−10.50**	−8.06*	2.87	4.11**
Adjusted R^2 (measure of goodness of fit)	0.45	0.26	0.12	0.29	0.45

* p-value < 0.05 (two-sided alternative).
** p-value < 0.01 (two-sided alternative).
*** p-value < 0.001 (two-sided alternative).

In this study, the compacted surfaces were prepared from powders of different size fraction. The roughness of surfaces was evaluated by image analysis. Fig. 3a and b shows the SEM images of 'rough' and 'smooth' surfaces with deposited particles at 100× magnification, Fig. 3c and d shows the SEM images of 'rough' and 'smooth' surfaces without deposited particles at 1000× magnification, Fig. 3e and f shows binary images of Fig. 3c and d which were used to calculate the surface porosity. The distance between asperities was expressed in two dimensions as surface area of troughs on the tablet's surface. The surface porosity of 'rough' surface is 9%, surface porosity of 'smooth' surface is 7.2%. The distribution of pore sizes on the surface is shown in Fig. 4.

For both the rough and the smooth surface, about 80% of the troughs have a surface area less than 20 μm^2 (Fig. 4), which is generally smaller than the apparent size of adhering particles (78 μm^2 for a 10 μm spherical particle). Hence, there is a low possibility that particles can be found in the troughs. But, the troughs and the cohering particles all differ from circular shape which opens the possibility that a part of a particle is positioned inside the troughs in an optimal configuration for cohesion, especially after the press-on procedure. The rough surface with some larger troughs may offer more possibilities for this arrangement. We also found a significant interaction between surface roughness and press-on force at three

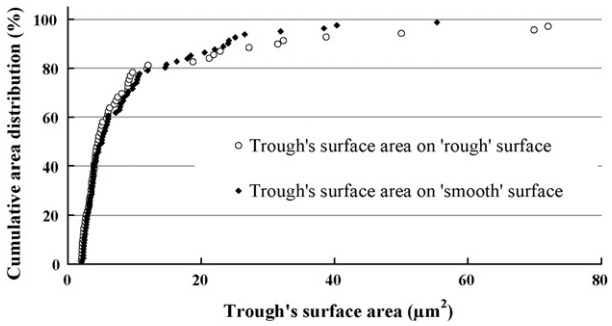

Fig. 4. Distribution of trough's surface area on substrate's surface.

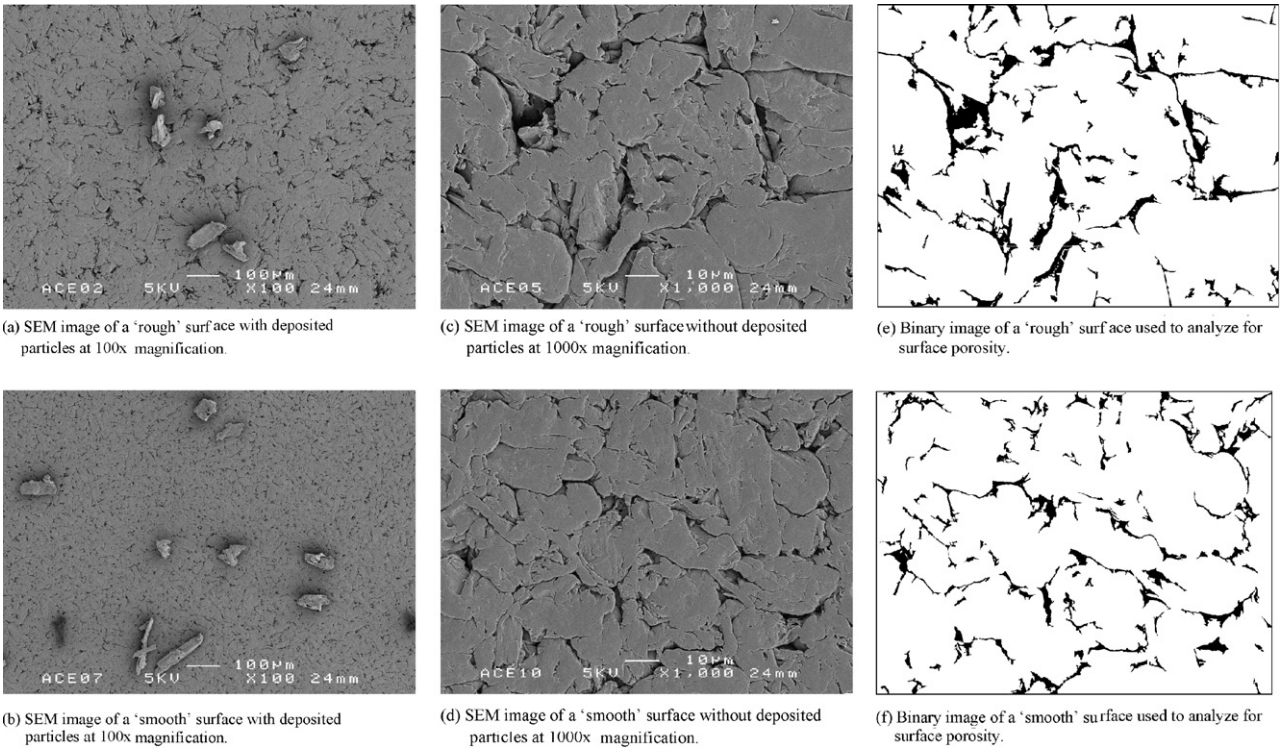

(a) SEM image of a 'rough' surface with deposited particles at 100x magnification.
(c) SEM image of a 'rough' surface without deposited particles at 1000x magnification.
(e) Binary image of a 'rough' surface used to analyze for surface porosity.
(b) SEM image of a 'smooth' surface with deposited particles at 100x magnification.
(d) SEM image of a 'smooth' surface without deposited particles at 1000x magnification.
(f) Binary image of a 'smooth' surface used to analyze for surface porosity.

Fig. 3. SEM and binary images of substrate's surface. (a) SEM image of a 'rough' surface with deposited particles at 100× magnification. (b) SEM image of a 'smooth' surface with deposited particles at 100× magnification. (c) SEM image of a 'rough' surface without deposited particles at 1000× magnification. (d) SEM image of a 'smooth' surface without deposited particles at 1000× magnification. (e) Binary image of a 'rough' surface used to analyze for surface porosity. (f) Binary image of a 'smooth' surface used to analyze for surface porosity.

spin-off speeds (1000, 3000 and 4000 rpm) which shows the importance of these parameters: the harder the particles are pressed on the rough surface, the more difficult it is to dislodge them. The quadratic effect of press-on time and press-on force is found to be significant at all spin-off speeds except at 3000 rpm. Because of the complete cofounding of quadratic effect of press-on time and press-on force, it is not possible to distinguish which effect is significant with the current experimental design. It is possible that both factors have a quadratic effect.

To obtain quantitative data on the cohesion force, it is necessary to map the centrifugal force with the corresponding particle detachment after each centrifugation. To enable the use of the force distribution concept, we calculated the adhesion force for each group of experiments on rough surfaces and for each group of experiments on smooth surfaces.

The introduction mentioned that the centrifugal force applied to different particles in a polydisperse sample is not uniform but depends on the particle size. As the centrifugal force is proportional to the third power of particle size, it is unrealistic to calculate centrifugal force based on an average particle size (i.e. arithmetic mean or median size) only. Therefore, we calculated the centrifugal force for each small particle size range obtained from laser diffraction analysis which is sufficient narrow that they may be considered as a monodisperse sample.

The volume based particle size distribution of the 38–53 μm fraction obtained by laser diffraction is shown in Fig. 1, open symbol. The median diameter (X_{50}) is 55 μm; X_{10} and X_{90} are 33 and 83 μm, respectively. The particle size distribution is larger than the sieve size used to obtain that fraction. The fact that the particles are larger than the largest sieve aperture used is explained by the particle shape. Avicel® PH-101 particles are rather fiber-shaped than spherical whereas the laser diffraction technique measures all particle dimensions and calculates volume distribution based on the assumption that the particles are spherical.

As the volume of particles is of critical importance in centrifugal force calculation, the volume equivalent diameter is used for data interpretation in this study. As the centrifuge forces will be analyzed in the form of number distribution, the number distribution of volume equivalent particle size was calculated based on laser diffraction distribution, result is shown in Fig. 1, solid symbol. The X_{10}, X_{50} and X_{90} are 12, 26 and 58 μm, respectively.

Centrifugal forces exerted on each particle size range at different centrifugation rate were calculated using Eq. (4) and results are shown in Table 4.

$$F_C = \frac{4\pi^3}{6^3 \times 10^2} \times \rho \times d_M^3 \times n^2 \times R_C \quad (4)$$

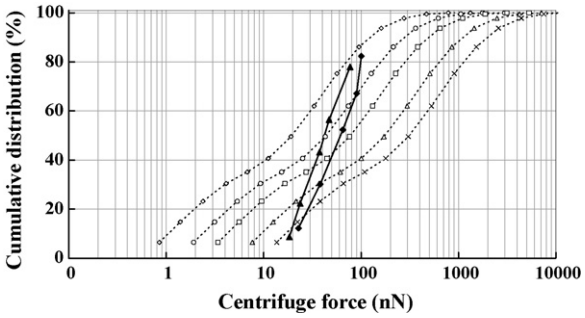

Fig. 5. Distribution of centrifugal forces and cohesion forces between MCC particles and MCC surfaces. Dotted line: centrifugal forces at 1000, 1500, 2000, 3000, 4000 rpm. (◊) 1000 rpm, (○) 1500 rpm, (□) 2000 rpm, (△) 3000 rpm, (×) 4000 rpm. Solid lines: cohesion forces between MCC particles and MCC surface. (♦) Cohesion force with 'rough' surface; (▲) cohesion force with 'smooth' surface

in which F_C is centrifugal force (N); ρ is true density of particle. In this case, $\rho = 1600\ kg/m^3$ for the MCC used (Zhang et al., 2003). d_M is arithmetic mean of upper and lower value of the size class; n centrifugal speed (rpm); R_C is centrifugal radius, which is the distance between rotation axis and the substrate surface. In this case, this distance is 0.1 m.

Fig. 5 shows the centrifugal force distribution curves for the polydispersed sample. The dotted line horizontally depicts the centrifugal force applied to each particle size fraction. The vertical axis shows the cumulative number distribution of the centrifugal force, which is derived from the particle size distribution. We obtained five curves (the dotted curves) to represent the centrifugal force distribution at the five centrifugal speeds: 1000, 1500, 2000, 3000 and 4000 rpm.

Based on the force distribution curves and the retention after each centrifugation (Table 2), the cohesion force is calculated by mapping the retention to the corresponding force curve. In principle, a particle is detached from the surface only if the centrifugal force applied to that particle exceeds the cohesion force of the particle and the surface. For example, in experiment number 1 (Table 2), at 1000 rpm centrifugal detachment, 17.8% of the particles were removed by the centrifugal force. This means that for this 17.8% of particles the centrifugal force is higher than the adhesion force and for the remaining 82.2% of particles the centrifugal force is lower than adhesion force. The centrifugal force distribution curve intersects the cohesion force curve at 82.2% on the y coordinate. The centrifugal force that corresponds to 82.2% on the 1000 rpm centrifugal force distribution curve is 100.6 nN (this value was calculated by fitting a linear correlation between the log of centrifugal force and cumulative force distribution). The procedure is the same

Table 4
Calculation of centrifuge forces (F_C) for different particle size range.

d (μm)	Cumulative distribution in number (%)	F_C (nN) at 1000 rpm	F_C (nN) at 1500 rpm	F_C (nN) at 2000 rpm	F_C (nN) at 3000 rpm	F_C (nN) at 4000 rpm
9.75	6.45	0.85	1.91	3.40	7.65	13.60
11.50	14.76	1.40	3.14	5.58	12.56	22.32
13.75	23.19	2.38	5.37	9.54	21.46	38.15
16.50	30.44	4.12	9.27	16.48	37.09	65.93
19.50	35.10	6.80	15.30	27.21	61.22	108.83
23.00	40.68	11.16	25.11	44.64	100.45	178.57
27.50	49.56	19.08	42.92	76.31	171.69	305.23
33.00	62.01	32.97	74.17	131.86	296.69	527.44
39.50	75.27	56.53	127.20	226.13	508.80	904.54
47.00	86.11	95.24	214.28	380.95	857.14	1523.80
56.00	93.74	161.09	362.46	644.38	1449.85	2577.50
67.00	97.83	275.89	620.76	1103.57	2483.03	4414.28
80.00	99.51	469.66	1056.74	1878.65	4226.96	7514.59
95.00	99.99	786.48	1769.57	3145.91	7078.29	12583.63
113.00	100.00	1323.58	2978.06	5294.32	11912.23	21177.29

Table 5
Calculation of cohesion force based on force distribution concept.

		Centrifuge speed (rpm)				
		1000	1500	2000	3000	4000
Rough surface	Retention (%)	82.38	67.15	52.34	30.21	12.23
	Adhesion force (nN)	100.59	89.80	64.96	38.16	22.79
Smooth surface	Retention (%)	78.02	56.47	43.27	22.37	8.69
	Adhesion force (nN)	77.19	46.96	37.47	23.72	18.39

for other detachment points. Results are shown in Table 5 and the detachment of MCC particles from rough and smooth surface is illustrated by the two solid lines in Fig. 5. The mean adhesion force of MCC particles with 'rough' and 'smooth' MCC surfaces are 63 ± 33 and 40 ± 23 nN, respectively.

Table 5 and Fig. 5 show that a high centrifugal speed is required to apply sufficient centrifugal detachment force to overcome low cohesion force of small particles. This is because the centrifugal force is proportional to the third power of the particle size and to the second power of the centrifugal speed. A higher increase in centrifugal speed is necessary to compensate the decrease in particle size. The cohesion force distribution is narrower than the centrifugal force distribution, the lower end of cohesion force curve intercept the lower end of centrifugal force curve at high centrifugal speed which correspond to the small particle size. The cohesion force decreases with decreasing particle size.

It should be noticed that the adhesion forces determined by the centrifuge method are of the same order of magnitude as the adhesion forces measured with AFM, although statistical comparison is non-appropriate due to the limited number of measurements by AFM. In the centrifugal detachment experiment, about 300 particles are deposited randomly on the substrate surface, and the experiment was carried out with four samples under the same conditions. Results generated from more than one thousand interactions may characterize the particle–surface adhesion in a powder mixture better.

Besides the advantages of the centrifuge method in characterizing particle–surface adhesion, there are still challenges regarding the effect of press-on force and press-on time and concerning the deformation of interacting material. In another image analysis of adhering particles using Morphologie G2 (Malvern Instrument, UK) (data not shown), the smallest 'apparent' surface area of the particle is about 800 μm^2. Even if the highest press-on force in this experiment (11912 nN at 3000 rpm) is applied to this particle, the 'apparent' pressure of 0.014 MPa is still much lower than the yield strength of microcrystalline cellulose (21 MPa) (Zuurman et al., 1999). Based on this observation, one may think that particle's surface or substrate's surface deformation are not likely to happen. However, the yield strength of a particle may differ from that of a surface and the possibility of plastic deformation, or flattening of asperities is still susceptible concerning the 'true' contact area. Due to the uneven nature of the particle's surface and of the substrate's surface, the interacting bodies only come in contact with the other at certain contact points resulting in a very small contact area. Even if a very small press-on force is applied on these tiny contact areas, the pressure may be high enough to exceed the yield strength of the material; this may cause plastic deformation of asperities and subsequently increase adhesion by increasing the contact area. Another possibility is the existence of areas with impurities or amorphous material on the particle or substrate's surface. These areas are normally soft and more susceptible to deformation, creating large contact surface areas with high adhesion. The influences of these surface properties have not yet been fully understood and are still challenging factors to interpret adhesion under press-on forces.

4. Conclusion

This paper shows that the force distribution concept can be applied in the calculation of adhesion force as studied by the centrifuge method. This concept is able to deal with the problem of polydispersity of the powder sample. The substrate's surface roughness, press-on force and press-on time affect the adhesion of the particle to a surface although the multiple linear regression model was not able to fully describe these factors. There are still challenges in clarifying the mechanism how the load condition (press-on force) influences the adhesion of particles to a surface.

Acknowledgement

The authors would like to thank Anko Eissens for the SEM images, TI Pharma for financial support for this research as part of D6-203-1: DeQuaPro project.

References

Begat, P., Morton, D.A.V., Staniforth, J.N., Price, R., 2004. The cohesive-adhesive balances in dry powder inhaler formulations I: direct quantification by atomic force microscopy. Pharm. Res. 21, 1591–1597.
Binnig, G., Quate, C.F., Gerber, C., 1986. Atomic force microscope. Phys. Rev. Lett. 56, 930.
Busscher, H.J., Dijkstra, R.J.B., Langworthy, D.E., Collias, D.I., Bjorkquist, D.W., Mitchell, M.D., Van Der Mei, H.C., 2008. Interaction forces between waterborne bacteria and activated carbon particles. J. Colloid Interface Sci. 322, 351–357.
De Boer, A.H., Hagedoorn, P., Gjaltema, D., Goede, J., Frijlink, H.W., 2003. Air classifier technology (ACT) in dry powder inhalation: Part 1. Introduction of a novel force distribution concept (FDC) explaining the performance of a basic air classifier on adhesive mixtures. Int. J. Pharm. 260, 187–200.
Derjaguin, B.V., Muller, V.M., Toporov, Y.P., 1975. Effect of contact deformations on the adhesion of particles. J. Colloid Interface Sci. 53, 314–326.
Dzyaloshinskii, I.E., Lifshitz, E.M., Pitaevskii, L.P., 1961. The general theory of van der Waals forces. Adv. Phys. 10, 165–209.
Hamaker, H.C., 1937. The London—van der Waals attraction between spherical particles. Physica 4, 1058–1072.
Hersey, J.A., 1975. Ordered mixing: a new concept in powder mixing practice. Powder Technol. 11, 41–44.
Hutter, J.L., Bechhoefer, J., 1993. Calibration of atomic-force microscope tips. Rev. Sci. Instrum. 64, 1868–1873.
Johnson, K.L., Kendall, K., Roberts, A.D., 1971. Surface energy and the contact of elastic solids. In: Proceedings of the Royal Society of London. Series A, Mathematical and Physical Sciences (1934–1990), vol. 324, pp. 301–313.
Krupp, H., 1967. Particle adhesion theory and experiment. Adv. Colloid Interface Sci. 1, 111–239.
Lam, K.K., Newton, J.M., 1991. Investigation of applied compression on the adhesion of powders to a substrate surface. Powder Technol. 65, 167–175.
Lam, K.K., Newton, J.M., 1993. The influence of the time of application of contact pressure on particle adhesion to a substrate surface. Powder Technology 76, 149–154.
Podczeck, F., Newton, J.M., 1995. Development of an ultracentrifuge technique to determine the adhesion and friction properties between particles and surfaces. J. Pharm. Sci. 84, 1067–1071.
Rumpf, H., 1990. Particle technology. In: Rumpf, H. (Ed.), Particle Technology. Chapman and Hall.
Salazar-Banda, G.R., Felicetti, M.A., Gonçalves, J.A.S., Coury, J.R., Aguiar, M.L., 2007. Determination of the adhesion force between particles and a flat surface, using the centrifuge technique. Powder Technol. 173, 107–117.
Saunders, R., 1991. The effect of particle agglomeration in pharmaceutical preparations. Statistician 40, 77–86.
Young, I., Gerbrands, J., Van Vliet, L., 1995. Techniques. Fundam. Image Process..

Zhang, Y., Law, Y., Chakrabarti, S., 2003. Physical properties and compact analysis of commonly used direct compression binders. AAPS PharmSciTech 4, E62.
Zimon, A.D., 1982a. Adhesion of Variously Shaped Particles to Rough Surfaces. Adhesion of Dust and Powder. United States, Plenum, New York, NY.
Zimon, A.D., 1982b. Methods for Determining Adhesive Force. Adhesion of Dust and Powder. United States, Plenum, New York, NY.
Zuurman, K., Van Der Voort Maarschalk, K., Bolhuis, G.K., 1999. Effect of magnesium stearate on bonding and porosity expansion of tablets produced from materials with different consolidation properties. Int. J. Pharm. 179, 107–115.